Numerical simulation of microfibrillated cellulose suspension in a pipe flow

Fuaad .P.A.[1], Agne Swerin[2], Fredrik Lundell[2], and Martti Toivakka[1]

[1] Åbo Akademi University, 20500 Turku, Finland
[2] Royal Institute of Technology KTH, SE-100 44 Stockholm, Sweden

ABSTRACT

Computational fluid dynamics (*CFD*) simulations are employed to investigate the flow behaviour of microfibrillated cellulose (*MFC*) suspensions at 0.5 % mass concentration in a pipe-flow geometry using OpenFOAM. A non-linear Navier-slip boundary condition is implemented to capture the boundary-slip as a function of the wall shear stress. The bulk viscosity of the *MFC* suspension is modelled using two successive power laws, with an identical exponent, and the consistency index transitioning based on the local shear rate. Preliminary results indicate that the pressure loss along the pipe is predicted reasonably accurately using the current computational model.

INTRODUCTION

Distinctive characteristics of Microfibrillated cellulose (*MFC*) based coatings such as robust mechanical properties, excellent barrier performance against oxygen, grease and oils establish it as a potential bio-based substitute for barrier applications. Considerable research effort is advanced in understanding the rheology of *MFC* suspensions due to diverse technological applications ranging from rheology modifiers[1] to functional materials.[2] In processing *MFC* coatings onto paperboard or thin films, a clear understanding of the rheological characteristics is essential. In contrast to macroscopic fibres in pulp suspensions, highly entangled microscopic fibrils in *MFC* suspensions leads to a complex flow behaviour, especially for higher solid contents. Such complex rheology includes yield stress, high viscosity even at low shear rates, highly shear thinning response, a tendency to develop water-rich boundary layer and an apparent boundary slip.[3]

COMPUTATIONAL METHODOLOGY

The governing partial differential equations (*PDE*) for an incompressible, isothermal fluid is the conservation of mass,

$$\nabla \cdot \mathbf{u} = 0 \tag{1}$$

and the conservation of the linear momentum,

$$\rho \left(\frac{\partial \mathbf{u}}{\partial t} + \nabla \cdot \mathbf{uu} \right) = -\nabla p + \nabla \cdot \tau \tag{2}$$

Here $\mathbf{u}$ denotes the velocity vector, p is the pressure and ρ is the density of the fluid. The rheology of *MFC* is described using a generalised non-Newtonian model where the fluid stress tensor (τ) is expressed as the product of an isotropic viscosity (μ) and the rate-of-strain tensor as,

$$\tau = 2\mu\left(\dot{\gamma}\right)\mathbf{S} \tag{3}$$

Here, $\mathbf{S} = 0.5\left(\nabla\mathbf{u} + \nabla\mathbf{u}^T\right)$ is the rate-of-strain tensor. For 0.5% mass-concentration

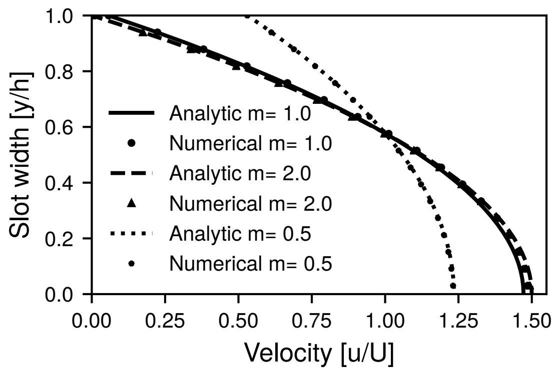

Figure 1. Validation of the non-linear slip model with results of Ferrás *et al.*[4]

MFC, the viscosity (μ) is a function of the shear rate, expressed as a combination of two power-laws with an identical flow index, but different consistency indices as suggested by Lauri *et.al.*[5] as

$$\mu = \begin{cases} 2.5 \times \dot{\gamma}^{-0.67} & \tau < \tau_{tr} \\ 1.9 \times \dot{\gamma}^{-0.67} & \tau > \tau_{tr} \end{cases} \quad (4)$$

The shear rate ($\dot{\gamma}$) is the second-invariant of the rate-of-strain tensor as $\dot{\gamma} = \sqrt{2\mathbf{S} : \mathbf{S}}$. Also, the transition shear rate (τ_{tr}) for Eq 4 is taken as 10 Pa. The Finite Volume Method (*FVM*) is employed as the numerical method to discretize the system of *PDE*s resulting from the governing equations using the OpenFOAM[6] framework. When considering boundary conditions at the wall, the no-slip condition ($\mathbf{u} = 0$) is substituted by a non-linear Navier-slip model dependent on the wall shear stress (τ_w) as,

$$\mathbf{u}_s = S\tau_w^m \quad (5)$$

Based on the optical coherence tomography measurement data of Lauri *et.al.*,[5] the coefficients for the non-linear Navier-slip model is set as $S = 8.3 \times 10^{-4}$ and $m = 1.84$. The accuracy of the non-linear slip boundary condition is verified against the analytical solutions of Ferrás *et al.*[4] in a slot geometry, as shown in Fig 1. The computational domain and the boundary conditions for the present study is illustrated in Fig 2. A uniform velocity profile corresponding to a constant mass flow-rate is prescribed along with zero gradient pressure boundary condition at the inlet. Along the lateral surfaces, a wedge type boundary condition is prescribed for each variable. A wedge type boundary condition approximates an axisymmetric flow by imposing equal fluxes with opposite signs in the azimuthal direction. For the outlet surface, the velocity field is prescribed zero gradient with a fixed pressure boundary condition.

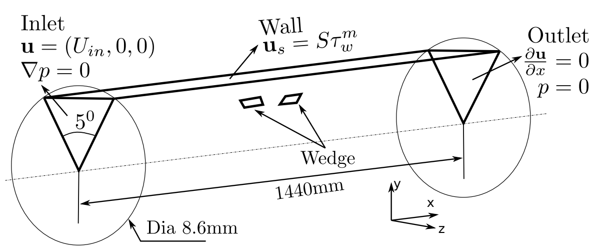

Figure 2. Computational domain with the boundary conditions.

RESULTS AND DISCUSSION

The mass-flow rate through the pipe was controlled by varying the inlet velocity. A total of 22 different mass-flow rates ranging from 6ml/min to 2118 ml/min were simulated with two different boundary conditions and rheology model combinations, as presented in Table 1.

Table 1. Simulation cases

	Model	Boundary Conditions	
		no-slip ($\mathbf{u} = 0$)	non-linear slip ($\mathbf{u}_s = S\tau_w^m$)
1	$\mu = 2.5 \times \dot{\gamma}^{-0.67}$	✓	
2			✓
3	Eq 4	✓	
4			✓

Fig 3 compares the pressure loss as a function of the mass-flow rate for *MFC* suspensions for the four different configurations considered. At low mass-flow rates ($Q < 500$ ml/min), the simulations with the no-slip boundary condition behave differently from the experimental results, particularly in the region where the pressure drop varies linearly with the mass flow

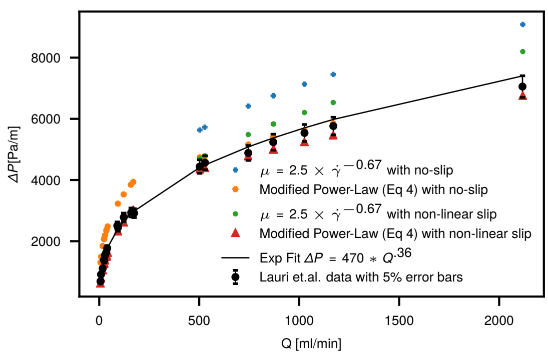

Figure 3. Comparison of pressure-drop for two different power-law models with no-slip and nonlinear Navier-slip boundary conditions.

rate. Also, the pressure drops predicted for both the power-laws using the non-linear slip model is identical for the cases with low mass-flow rates as the threshold of the shear stress for switching the consistency index is not attained. However, the relative importance of wall-slip reduces for higher mass-flow rates, where the effect of the slope transition of the power-law model is apparent. For the rheology model using Eq 4, at the maximum mass-flow rate considered (2118 ml/min), the difference between pressure-drop observed for a non-linear slip and a no-slip model is minimal.

In order to elucidate the role of slip in *MFC* pipe-flow simulations, the slip-velocity realized as a function of the mass-flow rate is presented in Fig.4. For higher mass-flow rates the slip-velocity is over-predicted by the power-law, and is clearly reflected as an overshoot in pressure losses, in comparison with the experimental results. The variation of the slip-velocity generated at the wall for higher mass-flow rates highlights the importance of considering the non-linear dependence of slip-velocity on wall-shear stress.

SUMMARY AND CONCLUSIONS

The current results compare a 0.5% *MFC* flow in pipe geometry using a power-law model with a single consistency index against a modified power law consisting of single exponent, but different consistency indices. These results provide a roadmap for developing more accurate models so that a comprehensive computational representation for processing *MFC* into coatings and films can be envisaged. However, more experimental data at higher mass concentrations is essential to generate meaningful insights to successfully model the rheology and the wall-slip.

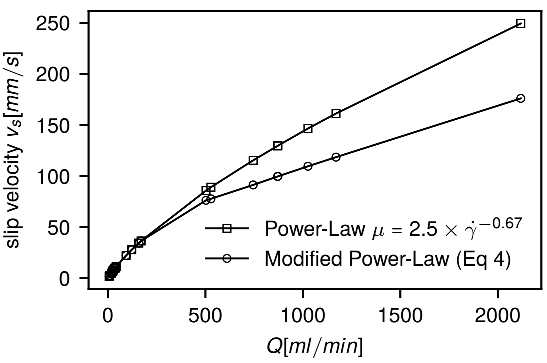

Figure 4. Comparison of slip-velocity for the two different power-law models.

ACKNOWLEDGEMENTS

This work was supported by KSLA Tandem Forest Values grant TFV I 2018 for the project "*SimNano - Numerical simulation of coating processes for nanocellulosic materials.*"

REFERENCES

1. K Dimic-Misic, PAC Gane, and J Paltakari. Micro-and nanofibrillated cellulose as a rheology modifier additive in cmc-containing pigment-coating formulations. *Industrial & Engineering Chemistry Research*, 52(45):16066–16083, 2013.

2. Vinay Kumar, Sven Forsberg, Ann-Christine Engström, Maristiina Nurmi, Britta Andres, Christina Dahlström, and Martti Toivakka. Conductive nanographite–nanocellulose coatings on paper. *Flexible and Printed Electronics*, 2(3):035002, 2017.

3. Behzad Nazari, Vinay Kumar, Douglas W Bousfield, and Martti Toivakka. Rheology of cellulose nanofibers suspensions: boundary driven flow. *Journal of Rheology*, 60(6):1151–1159, 2016.

4. LL Ferrás, JM Nóbrega, and FT Pinho. Analytical solutions for newtonian and inelastic non-newtonian flows with wall slip. *Journal of Non-Newtonian Fluid Mechanics*, 175:76–88, 2012.

5. Janne Lauri, Antti Koponen, Sanna Haavisto, Jakub Czajkowski, and Tapio Fabritius. Analysis of rheology and wall depletion of microfibrillated cellulose suspension using optical coherence tomography. *Cellulose*, 24(11):4715–4728, 2017.

6. Hrvoje Jasak. OpenFOAM: open source CFD in research and industry. *International Journal of Naval Architecture and Ocean Engineering*, 1(2):89–94, 2009.